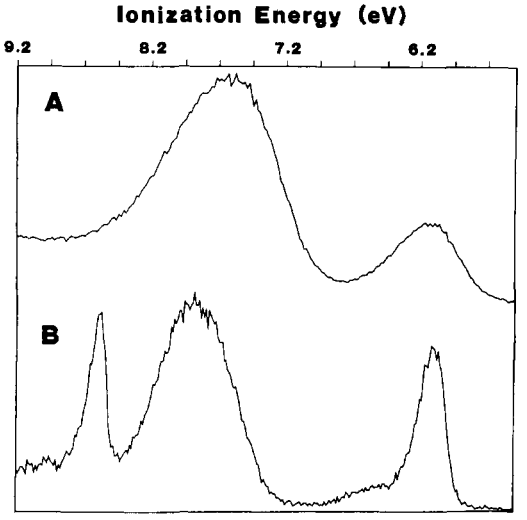

Figure 3. Close-up He I spectrum of the $W_2(O_2CCH_3)_4$ metal ionization region from thin-film (A) and gas-phase (B) experiments.

bonds are most likely occupied by the oxygen atoms of the neighboring complexes, as found in the single-crystal structures.

Valence ionizations of these complexes in the gas phase[6] and in thin films are shown in Figure 1. The general features of the gas-phase and thin-film spectra are seen to correlate closely. In the case of the molybdenum complex (Figure 1B), all of the major ionization features in the gas-phase spectrum are also observed in the thin-film spectrum with no significant relative ionization energy shifts (<0.1 eV).[17] Assignment of the leading ionization band to the δ and the second ionization band to the π (and perhaps the σ[18]) carries over to the solid from the gas-phase data. We do, however, observe a shoulder at $\approx$7.8 eV on the low binding energy side of the π band (Figure 2). This shoulder was reproduced for a variety of experimental conditions with this complex, and it was also observed for the formate analogue, $Mo_2(O_2CH)_4$. Comparison with the results of the W_2 study (vida infra) indicates that this shoulder corresponds to the σ ionization, which is destabilized from the π-ionization band by axial interactions in the thin film.

The analogous chromium compound (Figure 1A) also provides a close correlation of spectral features between the gas and thin-film spectra.[5] The leading ionization band in the gas-phase spectrum (8-9 eV) reveals broad overlapping ionization features assignable to predominantly metal orbitals.[19] This ionization band is shifted approximately 0.5 eV to lower energy relative to predominantly acetate ionizations in going to the thin film. The sensitivity of the energy of the leading ionization band of the chromium complex parallels the observed sensitivity of the chromium-chromium bond length to its environment, in particular to axial interactions.[11] The higher relative binding energy for this band in the gas-phase spectrum provides support for the shortened metal-metal distance found in the recent gas-phase electron diffraction structure.[13]

Comparison of the tungsten spectra in the gas phase and the thin film (Figure 1C) also reveals a one-to-one correspondence of ionization envelopes except for the sharp σ ionization at 8.56 eV in the gas-phase spectrum (Figure 3B).[9] The σ ionization is not independently observed in the thin-film spectrum. The increase in the intensity of the π-ionization region ($\sim$8 eV) relative to the δ-ionization region ($\sim$6 eV) in the thin film ($\sim$5:1) compared to the gas phase ($\sim$3:1) indicates that the σ ionization has shifted into the π-ionization band region. This observation is consistent with the disappearance of the sharp σ ionization with axial alkylation[15] and is understandable since the σ ionization would be expected to be more affected by axial interactions. This shift is also consistent with that proposed for the σ ionization of the molybdenum complex, indicating that these spectra have provided the first observation of the σ ionization in the region of the π ionization for a quadruply bonded Mo_2 dimer.

Acknowledgment. This research was made possible by funds from the Department of Energy (Division of Chemical Sciences, Office of Basic Energy Sciences, Office of Energy Research), the National Science Foundation, and the University of Arizona. We thank Dr. A. P. Sattelberger for supplying the sample of $W_2(O_2CCH_3)_4$.

(17) In addition to an alignment of the gas-phase and thin-film ionizations for maximum overlap of the primary ligand ionizations, the kinetic energy of the thin-film photoelectrons relative to the gas-phase spectra was also determined by defining the zero of kinetic energy as the onset of the electron cascade from the film. These two approaches agree to within a few tenths of an electronvolt.

(18) See Lichtenberger et al. (Lichtenberger, D. L.; Kober, E. M. *J. Am. Chem. Soc.* **1985**, *107*, 7199-7201 and references therein) for discussion of coincident π and σ ionizations.

(19) Lichtenberger, D. L., unpublished results and ref 6.

Heterogeneous Sonocatalysis with Nickel Powder

Kenneth S. Suslick* and Dominick J. Casadonte

School of Chemical Sciences
University of Illinois at Urbana—Champaign
Urbana, Illinois 61801

Received December 22, 1986

We have discovered that ultrasonic irradiation of Ni powder increases its activity as a hydrogenation catalyst by $>10^5$. In order to probe the origin of this dramatic enhancement, the surface composition has been examined. We find that ultrasonic irradiation of Ni powder causes remarkable changes in particle aggregation, surface morphology, and thickness of the surface oxide coating.

The use of high-intensity ultrasound to initiate or enhance both homogeneous and heterogeneous chemical reactions has been under intense investigation,[1-7] and a detailed understanding of the mechanism of *homogeneous* sonochemistry has recently been developed.[8] Our knowledge about the reaction conditions created

* Author to whom correspondence should be addressed.

(1) (a) Suslick, K. S. *Adv. Organomet. Chem.* **1986**, *25*, 73. (b) Suslick, K. S. *Modern Synth. Methods* **1986**, *4*, 1. (c) Suslick, K. S., Ed. *Ultrasound: Its Chemical, Physical and Biological Effects*; VCH Publishers: New York, 1987. (d) Boudjouk, P. *J. Chem. Ed.* **1986**, *63*, 427. (e) Margulis, M. A. *Ultrasonics* **1985**, *23*, 157.

(2) (a) Suslick, K. S.; Goodale, J. W.; Wang, H. H.; Schubert, P. F. *J. Am. Chem. Soc.* **1983**, *105*, 5781. (b) Suslick, K. S.; Schubert, P. F. *J. Am. Chem. Soc.* **1983**, *105*, 6042. (c) Suslick, K. S. In *High Energy Processes in Organometallic Chemistry*; Suslick, K. S., Ed.; ACS Symposium Series 333; American Chemical Society: Washington, DC, 1987; p 191.

(3) (a) Boudjouk, P. In *High Energy Processes in Organometallic Chemistry*; Suslick, K. S., Ed.; ACS Symposium Series 333: American Chemical Society: Washington, DC, 1987; pp 209-222. (b) Boudjouk, P.; Thompson, D. P.; Ohrbom, W. H.; Han, B. H. *Organometallics* **1986**, *5*, 1257. (c) Boudjouk, P. *Nachr. Chem., Tech. Lab.* **1983**, *31*, 797. (d) Boudjouk, P.; Han, B. H. *J. Org. Chem.* **1982**, *47*, 5030.

(4) (a) Luche, J. L. *Ultrasonics* **1987**, *25*, 40. (b) Petrier, C.; Dupuy, C.; Luche, J. L. *Tetrahedron Lett.* **1986**, *27*, 3149. (c) Petrier, C.; Barbosa, J. C.; Dupuy, C.; Luche, J. L. *J. Org. Chem.* **1985**, *50*, 910, 5761. (d) Luche, J. L.; Damiano, J. C. *J. Am. Chem. Soc.* **1980**, *102*, 7926.

(5) (a) Bonnemann, H.; Bogdanovic, B.; Brinkman, R.; He, D. W.; Spliethoff, B. *Angew. Chem., Intl. Ed. Engl.* **1983**, *22*, 728. (b) Suslick, K. S.; Johnson, R. E. *J. Am. Chem. Soc.* **1984**, *106*, 6856.

(6) (a) Lindley, J.; Mason, T. J.; Lorimer, J. P. *Ultrasonics* **1987**, *25*, 45. (b) Mason, T. J. *Lab. Pract.* **1984**, *33*, 13 and references therein.

(7) (a) Cioffi, E. A.; Prestegard, J. H. *Tetrahedron Lett.* **1986**, *27*, 415. (b) Moulton, K. J., Jr.; Koritala, S.; Frankel, E. N. *J. Am. Oil Chem. Soc.* **1983**, *60*, 1257. (c) Saracco, G.; Arzano, F. *Chim. Ind. (Milan)* **1968**, *50*, 314.

(8) (a) Suslick, K. S.; Cline, R. E., Jr.; Hammerton, D. A. *J. Am. Chem. Soc.* **1986**, *108*, 5641. (b) Suslick, K. S.; Hammerton, D. A. *IEEE Trans. Ultrason. Ferroelec., Freq. Cont.* **1986**, *33*, 143. (c) Suslick, K. S.; Hammerton, D. A. *IEEE Ultrason. Symp. Proc.* **1985**, *4*, 1116. (d) Suslick, K. S.; Gawienowski, J. W.; Schubert, P. F.; Wang, H. H. *Ultrasonics* **1984**, *22*, 33. (e) Suslick, K. S.; Gawienowski, J. W.; Schubert, P. F.; Wang, H. H. *J. Phys. Chem.* **1983**, *87*, 2299.

(9) (a) Mal'tsev, A. N. *Z. Fiz. Khim.* **1978**, *50*, 1641. (b) Lintner, W.; Hanesian, D. *Ultrasonics* **1977**, *14*, 21. (c) Boudjouk, P.; Han, B. H. *J. Catal.* **1983**, *79*, 489. (d) Han, B-H.; Boudjouk, P. *Organometallics* **1983**, *2*, 769.

0002-7863/87/1509-3459$01.50/0

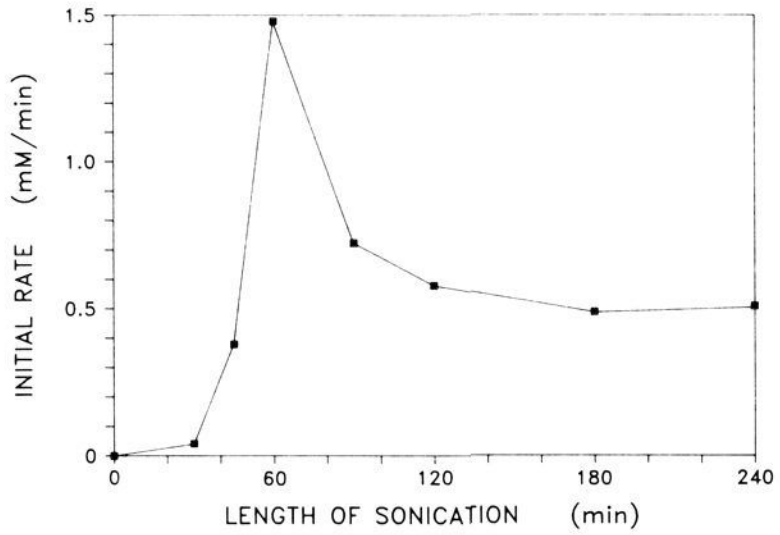

Figure 1. Initial rate of hydrogenation of 1-nonene vs. length of pretreatment of Ni powder by ultrasonic irradiation. Reactions run at 273 K and 1 atm of H_2 in octane.

by ultrasonic irradiation of liquid–solid interfaces, however, is much more limited.[1] When a liquid–solid interface is subjected to high-intensity ultrasound, acoustic cavitation[1] near the surface induces markedly asymmetric bubble collapse, which generates a high-speed jet of liquid directed at the surface.[10] The impingement of this jet and related shock waves can create a localized erosion (which produces highly reactive surfaces), improve mass transport, and cause particle fragmentation (which can substantially increase the surface area of friable solids,[11] e.g., supported catalysts). The effects of ultrasound on heterogeneous catalysis has had some exploration,[7,9] but the results have generally shown quite modest rate enhancements.[9a] There have been some recent reports, however, of large rate enhancements with supported metal catalysts;[7b,9d] the origins of such effects have not been delineated.

Simple Ni powder is an extremely inactive catalyst for hydrogenation of alkenes. Even after 2×10^4 min, no alkanes are detected with rapid stirring under 1 atm of H_2 at 273 K (i.e., <10 nM/min). In comparison under the same conditions, if the nickel is first irradiated with ultrasound,[12] 1-nonene is hydrogenated at millimolar per minute rates, as shown in Figure 1. Ultrasonic pretreatment of Ni powder for ≈1 h gives optimal activity, which decreases with longer irradiation. The hydrogenation activity is quite general and shows little dependence on choice of alkene (i.e., similar rates are observed with 1-nonene, 1-decene, *cis*-5-decene, *trans*-5-decene, cyclooctene, and cyclohexene); *no* reduction of ketones or aldehydes was observed.

Other methods for creating active Ni catalysts exist.[13] The thermal hydrogenation rates at 1 atm of H_2 and 273 K with high surface area Ni sponge (Raney Ni,[13a] Aldrich Chemicals, grade W-2) are comparable to those obtained with ultrasonically activated Ni powder. Compared to Raney Ni, however, our activated Ni powder is more selective (C–O double bonds are untouched), much easier to produce, and much simpler to handle (nonpyrophoric). Activation of Ni powders by H_2 at 150 °C and 10 atm will also generate reactive catalysts,[13b] which rapidly lose activity upon exposure to O_2.

One might initially assume that the increased activity might be due to increased surface area. This is *not* the case, however: ultrasonic irradiation of 5 μm Ni powder does not significantly decrease the particle size, even after several hours of irradiation. BET surface area measurements on Ni powders irradiated for increasing time show only a modest initial increase, followed by a *decrease* in total surface area: 0 min, 0.48 m^2/g; 15 min, 0.69

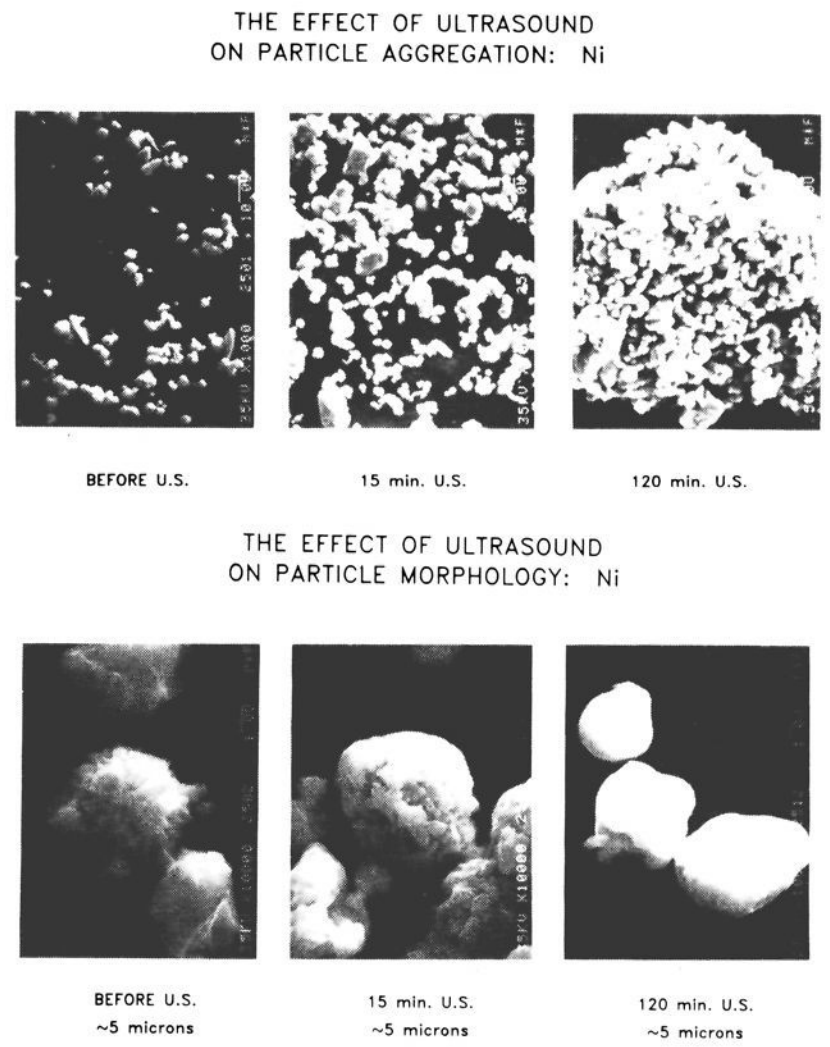

Figure 2. The effect of ultrasonic irradiation on particle aggregation and surface morphology of Ni powder. Note the magnification of the scanning electron micrograph in the upper spectra is tenfold less than in the lower spectra.

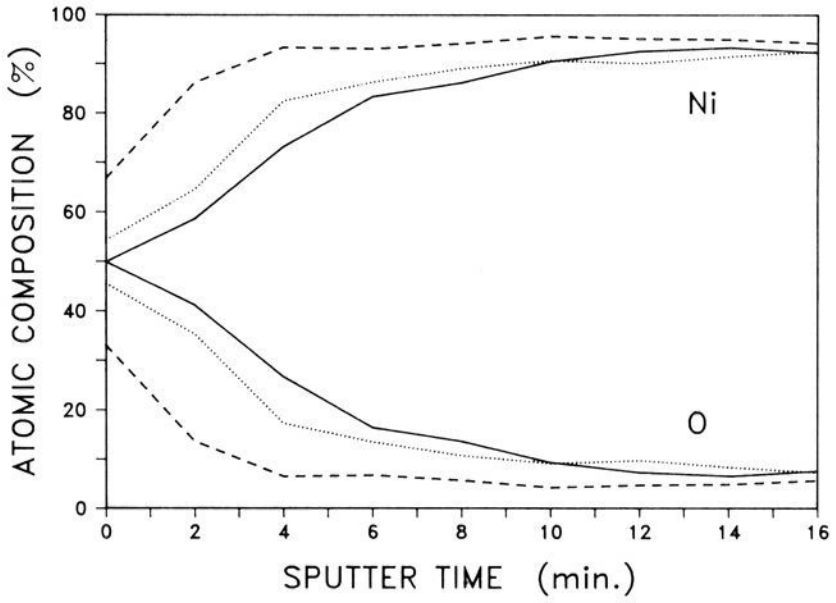

Figure 3. Surface composition depth profiles of Ni powder, as derived from Auger electron spectra obtained on a Physical Electronics 595 Multiprobe spectrometer with Xe^+ sputtering at 1 KeV and 18 $\mu A/cm^2$. Sputtering times correspond to an erosion rate of ≈25 Å/min. (—) Ni sample before ultrasound; (- - -) Ni sample after 1 h of ultrasonic irradiation. The sample was exposed to air for 8 min during preparation and loading. (•••) Ni sample after 1 h of ultrasonic irradiation, followed by intentional exposure to air for 13 min. Small amounts of surface carbon were also observed after ultrasonic irradiation.

(10) (a) Benjamin, T. B. *Philos. Trans.* **1966**, *A260*, 221. (b) Lauterborn, W.; Hentschel, W. *Ultrasonics* **1985**, *24*, 59. (c) Preece, C. M.; Hansson, I. L. *Adv. Mech. Phys. Surf.* **1981**, *1*, 199.

(11) (a) Suslick, K. S.; Casadonte, D. J.; Green, M. L. H.; Thompson, M. E. *Ultrasonics* **1987**, *25*, 56. (b) Suslick, K. S.; Green, M. L. H.; Thompson, M. E.; Chatakondu, K. *J. Chem. Soc., Chem. Commun.*, in press.

(12) All sonications were performed with a Heat Systems-Ultrasonics W375 cell disruptor with a titanium immersion horn at acoustic intensities of ≈50 W/cm^2 at 20 KHz, as described in detail elsewhere.[2] Irradiation in a low-intensity ultrasonic cleaning bath does give hydrogenation, but at greatly reduced rates. Hydrogenation reactions were carried out at 273 K under 1 atm of H_2. In a typical reaction, 1 g of Ni powder (200 mesh, EM Science, Cherry Hill, NJ 08034) was added to a 10% solution of alkene in octane. Products were analyzed by GC–MS and capillary GC with heptane as internal standard.

(13) (a) Fieser, L. F.; Fieser, M. *Reagents for Organic Synthesis*; Wiley: New York, 1967; Vol. 1, pp 723–731. (b) Thomas, C. L. *Catalytic Processes and Proven Catalysts*; Academic: New York, 1970; pp 126–133. (c) Somorjai, G. A. *Chemistry in Two Dimensions: Surfaces*; Cornell University Press: Ithaca, NY 1981; pp 445–447. (d) White, J. M. *J. Phys. Chem.* **1983**, *87*, 915. (e) Rieke, R. D.; Burns, T. P.; Wehmeyer, R. M.; Kahn, B. E. In *High Energy Processes in Organometallic Chemistry*; Suslick, K. S., Ed.; ACS Symposium Series 333: American Chemical Society: Washington, DC, 1987; pp 223–245.

m^2/g; 120 min, 1.00 m^2/g; 240 min, 0.57 m^2/g; with errors of ±5%.

Scanning electron micrographs were obtained on Ni samples irradiated for 0, 15, and 120 min, as shown in Figure 2. As the malleable particles are irradiated, profound changes in particle aggregation and morphology are observed. The surface of our Ni powder is initially highly crystalline, but upon sonication the surface is smoothed quite rapidly. At the same time, the extent of aggregation increases dramatically. We believe that both effects are due to interparticle collisions driven by the turbulent flow created by the ultrasonic field. The increase aggregation accounts for the eventual decrease in the observed surface area and probably also causes the small diminution in activity observed after lengthy sonication.

This change in surface morphology is associated with a dramatic change in surface composition. Auger electron spectra depth profiles were obtained on Ni samples before and after sonication, as shown in Figure 3. Initially, a thick oxide coat is found (with a surface Ni/O ratio of 1.0) extending ≈250 Å into the particle. After 1 h of ultrasonic irradiation in octane, the oxide layer is *much* thinner (<50 Å, with a surface Ni/O ratio of 2.0). In fact, most of the oxide layer in the irradiated sample is due to its air exposure during sample transfer; the oxide coating is fully reestablished after ≈15 min of air exposure. It is likely that the origin of our observed sonocatalytic activity comes from the removal (through interparticle collisions) of the surface oxide layer normally found on Ni powders. A clean Ni surface is an active catalyst;[13] nickel powder with its usual surface oxide coating is not.

Acknowledgment. Special thanks are due Dr. Frank Scheltens for assistance with the scanning electron micrographs and Nancy Finnegan for the Auger electron spectra; both analyses were carried out in the Center for Microanalysis of Materials, University of Illinois, which is supported by the U.S. Department of Energy under Contract DE-AC 02-76ER 01198. We also thank Brian Borglum and Professor R. C. Buchanan for their aid in obtaining surface area measurements. The support of the National Science Foundation (CHE 8319929) is greatly appreciated. K.S.S. gratefully acknowledges the receipt of an N.I.H. Research Career Development Award and of a Sloan Foundation Research Fellowship.

Esperamicins, a Novel Class of Potent Antitumor Antibiotics. 2. Structure of Esperamicin X

Jerzy Golik,*[1a] Jon Clardy,[1b] George Dubay,[1a] Gary Groenewold,[1a] Hiroshi Kawaguchi,[1c] Masataka Konishi,[1c] Bala Krishnan,[1a] Hiroaki Ohkuma,[1c] Kyo-ichiro Saitoh,[1c] and Terrence W. Doyle[1a]

Bristol-Myers Pharmeceutical Research and Development Division, Wallingford, Connecticut 06492, Department of Chemistry, Cornell University, Ithaca, New York 14853, Bristol-Myers Research Institute, Tokyo Meguro, Tokyo, Japan

Received November 28, 1986

Recently we have described the isolation and partial structure elucidation of esperamicins A_1 and A_2 which are produced by cultures of *Actinomadura verrucosospora* (BBM1675, ATCC 39334)[2,3a,b] and are characterized by broad spectrum antitumor activity in murine systems.[4] To our knowledge they are the most potent antitumor agents yet discovered. The esperimicins are produced as a complex of related compounds which we have resolved into a number of components, A_1, A_2, A_{1b}, A_3, A_4, B_1, and B_2.[5,6] In addition to these bioactive metabolites, we have also isolated esperamicin X (**1**), an inactive compound coproduced by the organism. Similarities in the physical properties of **1** with the bioactive metabolites have led us to undertake the structure elucidation of **1** (Figure 1).

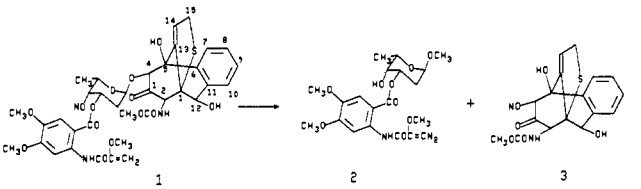

Figure 1. Methanolysis of esperamicin X—stereochemistry of tetracyclic core arbitrarily chosen.

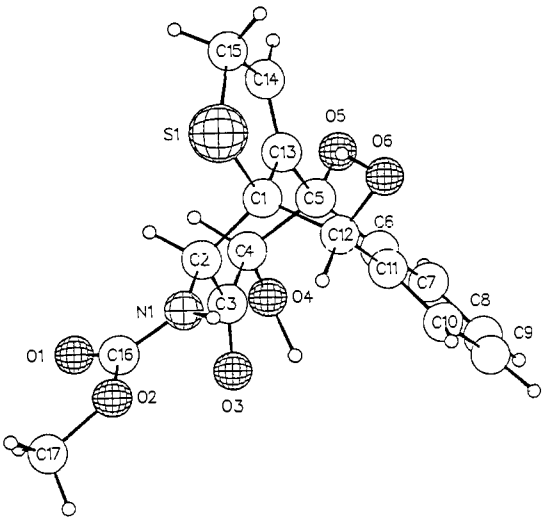

Figure 2. Computer-generated perspective drawing of **3**.

Compound **1** was isolated as a white crystalline solid, mp 182–184 °C, $[\alpha]_D$ −36° (*c* 0.5, $CHCl_3$). Its molecular formula was established as $C_{36}H_{40}N_2O_{14}S$ by using FAB mass spectroscopy (MW 756) and elemental analysis. The IR spectrum of **1** had bands characteristic of hydroxyl, ester, amide, and enol ether functions.[7] The UV spectrum of **1** was similar to that of esperamicin A_1.[8] Examination of the ^1H and ^{13}C NMR spectra of **1** showed the presence of numerous resonances observed in the spectrum of esperamicins A_1, A_{1b}, and A_2 and encouraged a more thorough analysis.[9]

(1) (a) Bristol-Myers Pharmeceutical Research and Development Division. (b) Cornell University. (c) Bristol-Myers Research Institute.

(2) The producing organism was collected at Pto Esperanza, Misiones, Argentina. Consequently we have given the trivial name of esperamicin to compounds isolated from the complex.

(3) (a) Konishi, M.; Saitoh, K.; Ohkuma, H.; Kawaguchi, H. Japan Kokai 84-232 094, Dec 26, 1984. (b) Konishi, M.; Ohkuma, H.; Saitoh, K.; Kawaguchi, H.; Golik, J.; Dubay, G.; Groenewold, G.; Krishnan, B.; Doyle, T. W. *J. Antibiot.* 1985, *38* 1605–1609. (c) Kiyoto, S.; Nishikawa, M.; Terano, H.; Kohsaka, M.; Aoki, H.; Imanaha, H.; Kawai, Y.; Uchida, I.; Hashimoto, M. *J. Antibiot.* **1985**, *38*, 840–848. (d) Bunge, R. H.; Hurley, T. R.; Smitka, T. A.; Willmer, N. E.; Brankiewicz, A. J.; Steinman, C. E.; French, J. C. *J. Antibiot.* **1984**, *37*, 1566–1571. (e) Lee, M. D.; Greenstein, M.; Labeda, D. P. Eur. Patent Appl. 0 182 152, May 28, 1986.

(4) Esperamicins A_1, A_{1b}, and A_2 are active in a number of murine tumor models (P388, B16, M5076, etc.) at doses in the 100 ng/kg/injection range.[6]

(5) Manuscripts detailing the taxonomy and fermentation of BBM1675 are in preparation: Claridge, C. A.; Forenza, S.; Hatori, M.; Kawaguchi, H.; Kimball, D. L.; Lam, K. S.; Miyaki, T.; Titus, J. A.; Tomita, K.; Veitch, J. A., unpublished results, 1987.

(6) A manuscript detailing the isolation and biological activities of these components is in preparation: Bradner, W. T.; Forenza, S.; Golik, J.; Kawaguchi, H.; Konishi, M.; Matson, J. A.; Ohkuma, H.; Saitoh, K., unpublished results, 1987.

(7) IR bands at 3400, 2940, 1740 (sh), 1730, 1685, 1610, 1595, 1525, 1450, 1365, 1350, 1310, 1250, 1210, 1155, 1180, 1025, 1000, 785, 760, and 755 cm^{-1}.

(8) UV bands in methanol at λ_{max} (nm) 323 (ε 10 900), 285 (ε 10 500), and 253 (ε 25 900).

0002-7863/87/1509-3461$01.50/0